

UCLA

UCLA Previously Published Works

Title

Early dietary restriction in rats alters skeletal muscle tuberous sclerosis complex, ribosomal s6 and mitogen-activated protein kinase

Permalink

<https://escholarship.org/uc/item/1q003329>

Authors

Calkins, Kara L
Thamotharan, Shanthie
Dai, Yun
et al.

Publication Date

2018-06-01

DOI

10.1016/j.nutres.2018.03.013

Peer reviewed



Published in final edited form as:

Nutr Res. 2018 June ; 54: 93–104. doi:10.1016/j.nutres.2018.03.013.

Early Dietary Restriction in Rats Alters Skeletal Muscle Tuberous Sclerosis Complex, Ribosomal s6 and Mitogen-Activated Protein Kinase

Kara L. Calkins^a, Shanthie Thamotharan^a, Yun Dai, Bo-Chul Shin^a, Satish C. Kalhan^b, and Sherin U. Devaskar^{a,*}

^aDepartment of Pediatrics, Division of Neonatology & Developmental Biology, Neonatal Research Center of the UCLA Children's Discovery and Innovation Institute, David Geffen School of Medicine UCLA, 10833 Le Conte Avenue, Los Angeles, CA 90095-1752

^bDepartment of Pathobiology, Lerner Research Institute, Cleveland Clinic, 9620 Carnegie Avenue, Cleveland, Ohio 44106

Abstract

Intra-uterine growth restriction is linked to decreased lean body mass and insulin resistance. The mammalian target of rapamycin (mTOR) regulates muscle mass and glucose metabolism; however, little is known about maternal dietary restriction and skeletal muscle mTOR in offspring. We hypothesized that early dietary restriction would decrease skeletal muscle mass and mTOR in the suckling rat. To test this hypothesis, *ab libitum* access to food or dietary restriction during gestation followed by postnatal cross-fostering to a dietary restricted or *ad libitum* fed rat dam during lactation, generated four groups: control (CON), intra-uterine dietary restricted (IUDR), postnatal dietary restricted (PNDR), and IUDR+PNDR (IPDR). At day 21, when compared to CON, the IUDR group demonstrated “catch-up” growth but no changes were observed in the mTOR pathway. Despite having less muscle mass than CON and IUDR ($p < 0.001$), IPDR and PNDR mTOR rats remained unchanged. IPDR and PNDR (p)-tuberous sclerosis complex (TSC) 2 was less than the IUDR group ($p < 0.05$). Downstream, IPDR and PNDR's phosphorylated (p)-ribosomal s6 (rs6)/rs6 was less than CON ($p < 0.05$). However, male IPDR and PNDR's p-mitogen activated protein kinase MAPK/MAPK were greater than CON ($p < 0.05$) without a change in p90 ribosomal s6 kinase (p90RSK). In contrast, in females, MAPK was unchanged but IPDR p-p90RSK/p90RSK was less than CON ($p = 0.01$). In conclusion, IPDR and PNDR reduced skeletal muscle mass but did not decrease mTOR. In IPDR and PNDR, a reduction in TSC2 may explain why mTOR was unchanged; whereas, in males, an increase in MAPK with a decrease in rs6 may suggest a block in MAPK signaling.

*Corresponding Author: 10833, Le Conte Avenue, MDCC-22-402, Los Angeles, CA, 90095-1752, Ph. No.: 310-825-9357, FAX No.: 310-206-4584; sdevaskar@mednet.ucla.edu.

Publisher's Disclaimer: This is a PDF file of an unedited manuscript that has been accepted for publication. As a service to our customers we are providing this early version of the manuscript. The manuscript will undergo copyediting, typesetting, and review of the resulting proof before it is published in its final citable form. Please note that during the production process errors may be discovered which could affect the content, and all legal disclaimers that apply to the journal pertain.

Keywords

muscle; skeletal; rats; diet reducing; fetal growth retardation; TOR serinethreonine kinase; mitogen-activated protein kinase phosphatases

1. Introduction

Intra-uterine and postnatal growth restriction due to inadequate dietary intake is a world-wide problem which results in growth stunting and early childhood mortality [1, 2]. With the increased survival of growth restricted infants, the development of non-communicable chronic conditions such as diabetes, obesity, hypertension, dyslipidemia, and coronary artery disease have increased [1–5]. Stunted growth during infancy and childhood predicts the later onset of the metabolic syndrome [1–5]. We and others have employed animal models mimicking this situation by exposure to prenatal and postnatal dietary restriction [6–12]. We have shown that the adult male rat and mouse offspring subjected to this insult develop glucose intolerance, central adiposity, and dyslipidemia [8–10]. In contrast, the female offspring expresses glucose intolerance during pregnancy [11]. During prenatal dietary restriction, placental transfer of branched chain amino acids and other nutrients are reduced providing a mechanism by which fetal growth restriction occurs [12–15]. Similarly, maternal postnatal protein restriction causes a reduction in the offspring's amino acid profiles and postnatal growth restriction [15]. These dietary insults disrupt myogenesis and reduce lean body mass [1,4,5]. Since skeletal muscle is the principal tissue for insulin-mediated whole-body glucose disposal, understanding how intra-uterine and postnatal growth restriction alter skeletal muscle development is clinically relevant [1,4,5].

The mammalian target of rapamycin (mTOR) plays a crucial role in mediating muscle growth and metabolic disease [16–21]. mTOR acts as an energy sensor that is highly responsive to circulating amino acids, growth factors, glucose, and adenosine monophosphate-activated protein (AMP) kinase [19,20]. mTOR regulates the cell cycle, ribosomal biogenesis, mRNA translation, autophagy, and cell growth and differentiation [19,20]. Perturbed mTOR signaling has been linked to adult onset sarcopenia, intramuscular lipid accumulation, and the metabolic syndrome [16–20]. mTOR has two downstream mediators: 1) p70S6kinase 1 (S6K1) and 2) 4E binding protein-1 (4EBP1). S6K1 mediates ribosomal biogenesis by regulating ribosomal S6 (rs6) protein. 4EBP1, when phosphorylated, releases the eukaryotic translational initiation factor-4E (eIF4E). EIF4E, in turn, regulates the 7-methyl-guanosine 5'-cap structure, m7GpppX (where X is any nucleotide) mediated mRNA translation. This is a rate-limiting component of the eukaryotic translation apparatus, which is involved in the mRNA-ribosome binding step of eukaryotic protein synthesis that is required for translating mRNAs into polypeptides. Upstream, tuberous sclerosis complex (TSC) 1 (encodes hamartin) and TSC 2 (encodes tuberin) heterodimerize to negatively regulate mTOR. TSC complexes are inactivated by the insulin/insulin-like growth factor (IGF) related signaling molecules. This inactivation of the TSC complex activates the mTOR signaling pathway, thereby mediating the growth promoting effect of insulin and IGF.

Another pathway stimulated by growth factors is the intracellular mitogen activated protein kinase (MAPK) pathway, which includes upstream MAP3K and MAP2K and downstream p90 ribosomal S6 kinase (p90RSK) followed by rs6 protein [22]. These proteins facilitate skeletal muscle ribosomal biogenesis, cellular proliferation, differentiation, survival and death [22]. Activated MAPK inhibits TSC2 activation releasing inhibition on the mTOR pathway.

To date, little is known about the effect of intra-uterine and postnatal dietary restriction on skeletal muscle mTOR signaling. Accordingly, this study's objective was to investigate the effect of maternal dietary restriction on the offspring's skeletal muscle mass and mTOR. In 21-day (d) old rats, we hypothesized that maternal dietary restriction would decrease skeletal mass and downregulate mTOR in comparison to offspring born to mothers who received a standard diet. This hypothesis is based on the fact that mTOR is highly responsive to nutrient intake and plays a major role in controlling muscle mass [16–21]. To test this hypothesis, we used a prenatal and postnatal dietary restricted rat model and employed four experimental groups, control with *ad libitum* exposure to diet and water (CON), intra-uterine dietary restriction (IUDR), postnatal dietary restriction (PNDR) and a combination of prenatal and postnatal dietary restriction (IPDR). We then examined the early stage hind limb skeletal muscle of males and females. This research will help advance our understanding of how dietary restriction during periods of critical development alter skeletal muscle development and why fetal growth restriction is associated with adult-onset insulin resistance [1–5].

2. Methods and Materials

2.1 Animals

Sprague-Dawley rats (Charles River Laboratories, Hollister, CA) were housed in individual cages, exposed to 12-hour light-dark cycles at 21–23°C, and allowed *ad libitum* access to standard rat chow (Diet 7013, Envigo, Madison WI) [23]. The diet contained the following: energy 3.1 kcal/kg, (calories from protein 23%, from fat 18%, and from carbohydrate 59%), crude protein 18%, fat (ether extract) 6.2%, carbohydrate (available) 45%, crude fiber 4%, neutral detergent fiber 13.6%, and ash 6.2%. The National Institutes of Health guidelines were followed. All protocols were approved by the Animal Research Committee at the University of California, Los Angeles (protocol no. 1999-104-53E).

2.2 Maternal dietary restriction model

One group of pregnant rats received approximately 50% of their daily food intake (11 g/d) from gestational d11 through d21, constituting the period of mid- to late gestation. In contrast, the age-matched control pregnant rats received *ad libitum* access to standard rat chow (approximately 22 g/d) [8–11,24]. Both these groups had free access to drinking water. The rats were monitored on a daily basis to ensure against excessive (>10%) maternal weight loss during pregnancy.

2.3 Postnatal animal maintenance

Pups were randomly selected from a group of 60–80 pups (6–8 different litters). At birth, the litter size was culled to six. Each pup in a group came from a different litter. The newborn rats born to the prenatally dietary restricted mothers were cross-fostered to be reared by either a dam that continued to be dietary restricted (approximately 20 g/d) during lactation (IPDR) or a control mother with *ad libitum* access to standard rat chow (IUDR). Similarly, newborn pups born to control dams were cross-fostered to be reared by either a mother who was dietary restricted (PNDR) through lactation (approximately 20 g/d) or a control dam with *ad libitum* access to standard rat chow (CON) (approximately 40 g/d) [8–11,24]. This study design led to four groups, CON, IUDR, IPDR and PNDR of rat pups reared by the dams.

2.4 Anthropometric measurements

Body weights at postnatal d2 and d21 were recorded. At postnatal d21, nose-tail lengths were measured. Pups were then anesthetized with inhaled isoflurane, and organ, adipose tissue, and hind limb skeletal muscle (gastrocnemius and soleus) were harvested and weighed.

2.5 Plasma Analyses

Intra-cardiac blood was collected and blood cells were separated from plasma. Glucose was measured by HemoCue Glucose 201 (HemoCue America, Brea CA). Plasma was frozen at -70°C for future analyses. Plasma insulin-like growth factor (IGF)-1 concentrations were assessed by a validated, “in-house” enzyme-linked immunosorbent kit developed at the University of California, Los Angeles [25]. The amino acid profile was measured by gas chromatography-mass spectrometric analysis, as previously described [26].

2.6 Antibodies

Rabbit polyclonal anti-mTOR, anti-phosphorylated (p) mTOR^{ser2448}, anti-S6K1, anti-p-S6K1^{thr389}, anti-rS6, anti-p-rS6^{ser235/236}, anti-4EBP1, anti-p-4EBP1^{ser65}, anti-EIF4E, anti-p-EIF4E^{ser209}, anti-TSC1, anti-TSC2, anti-p-TSC2^{ser1462}, anti-p44/42 MAPK, anti-p-MAPK^{thr202/tyr204}, anti-RSK1/RSK2/RSK3, and anti-p-p90RSK^{ser380} were obtained from Cell Signaling (Beverly, MA). Anti-vinculin antibody was purchased from Sigma Chemical (St. Louis, MO).

2.7 Western Blot Analysis

Postnatal rat skeletal muscle was separated from surrounding tissues, snap-frozen in liquid nitrogen, and stored at -70°C . As previously described, skeletal muscle was powdered under liquid nitrogen and suspended in three volumes of cell lysis buffer (Cell Signaling Technology, Beverly, MA) [24]. Samples were sonicated with a hand-held homogenizer for 1–2 minutes and then homogenized with a tight-fitting Potter Elvehjem homogenizer [24]. Finally, samples were centrifuged at 10,000 rpm at 4°C for ten minutes and stored at -70°C for future analysis [24].

Fifty-100 µg of skeletal muscle protein homogenates were separated by SDS-PAGE and transferred to nitrocellulose membranes. As previously described, membranes were treated with 5% nonfat dry milk in phosphate-buffered saline containing 0.1% Tween 20 for one hour and then incubated with primary antibodies (1:500 for anti-p-p90RSK^{ser380} and 1:1000 dilution for remaining antibodies) at room temperature for either one hour or overnight at 4°C. Vinculin (1:4000-1:7000 dilution) served as the internal control to overcome inter-lane loading variability [24]. The membranes were then washed three times with 0.1% Tween 20 and probed with the appropriate secondary horseradish peroxidase-conjugated antibody (1:2500) for one hour at room temperature [24]. Membrane protein bands were visualized with the enhanced chemiluminescence method (Amersham Biosciences, Piscataway, NJ) after extensive washing. Quantification of protein bands was performed using the Image Quant System.

2.8 Skeletal muscle morphology

Animals were perfused with 4% formaldehyde solution via a syringe pump (KD Scientific, Holliston, MA). The soleus was collected, paraffin embedded and sectioned (8-µm thickness) using a Leica RM 2235 vibratome (Nussloch, Germany). Hematoxylin/eosin staining was performed, and sections were mounted and visualized using a Nikon Eclipse E-600 microscope (Nikon, Melville, NY) (20× magnification) that was equipped with a cooled, charge-coupled device camera (CoolSNAP HQ Monochrome; Roper Scientific, Tucson, AZ). Images were taken using the Metamorph Meta-imaging analysis software (Molecular Devices, Sunnyvale, CA). Muscle bundle and fiber cross-sectional area were assessed by using ImageQuant TL Software (GE Healthcare Life Sciences, Pittsburgh, PA); the cross-sectional areas for at least two-six bundles and fibers for three different animals were measured and then averaged for comparison between groups. Oil Red staining was also performed for descriptive analysis. Images were acquired using the same microscope (40× magnification).

2.9 Statistical Analyses

Day 2 CON and IUDR body weights were compared using the Student t-test. For comparisons at d21, the four experimental groups and two genders were compared using a two-way analysis of variance model with a post-hoc Tukey test. Aspartic and glutamic acid values were log transformed for normality. For the analysis of proteins only, the four groups (CON, IUDR, IPDR, and PNDR) for each sex were compared using a one-way analysis of variance model with a post-hoc Tukey test. Using a one-way ANOVA and assuming a standard deviation of 13 and means of 100 (CON), 95 (IUDR), 75 (IPDR), and 85 (PNDR); a sample size of 24 (n=6 per group) provided 80% power, assuming a two-sided alpha of 0.05, to detect a difference among the group means. We believed these assumptions and differences were reasonable based on our previous work [24]. P<0.05 was considered statistically significant to reject the null hypothesis. All results are presented as means ± SEM.

3. Results

3.1 Body Weights

At postnatal d2, male and female IUDR body weights were less than CON ($p < 0.001$ for each) (Figure 1). At postnatal d21, while the male IUDR demonstrated some “catch-up growth,” IUDR weighed less than CON ($p < 0.001$). The body weights of the female IUDR group were comparable to CON. In contrast, both male and female IPDR and PNDR groups weighed approximately 60–70% less than CON and IUDR ($p < 0.001$ for all) (Figure 2).

3.2 Anthropometric Measurements

Postnatal d21 IUDR males and females experienced “brain sparing” when compared to CON, as noted by similar brain weights. While male IUDR nose-tail length and organ weights (liver, kidney, pancreas, gastrocnemius) weighed less than CON males ($p < 0.05$ all), adipose tissue and soleus were comparable to CON males. Female IUDR nose-tail lengths were comparable to CON, but IPDR and PNDR nose-tail lengths were less than CON and IUDR ($p < 0.05$ for all). Most female IUDR organ weights were either comparable to female CON or greater than male IUDR (liver, kidney, pancreas, white adipose tissue and gastrocnemius) ($p < 0.05$ all). Specifically, female IUDR liver was 40% and 30% heavier when compared to female CON ($p < 0.001$) and male IUDR ($p = 0.002$). Female IUDR white adipose tissue was 150% heavier than male IUDR ($p < 0.001$) (Table 1).

When expressed as a fraction of body weight, no difference was seen overall in all male IUDR organ weights and most IUDR female organ weights compared to their respective CON groups. However, female IUDR liver was greater than female CON and male IUDR ($p < 0.001$ for each). Female white adipose tissue was 40% heavier than male IUDR ($p = 0.001$) (Table 1).

In contrast to IUDR, both IPDR and PNDR’s nose-tail lengths and organ weights were less than CON and IUDR ($p < 0.05$ for all). Analyses of sex differences revealed that the female PNDR brown adipose tissue and gastrocnemius were greater than male PNDR ($p < 0.05$). However, when organ weights were expressed as a fraction of the respective body weights, most IPDR and PNDR measurements were less than, with the exception of an increase in nose-tail length and brain weight, their respective sex-matched CON and IUDR groups. In both groups, white adipose tissue was difficult to detect, making quantification unattainable (Table 1).

3.3 Metabolites and Growth Factors

While plasma glucose was not different in either male or female IUDR versus CON, plasma IPDR and PNDR glucose was less than CON and IUDR ($p < 0.05$ for all). Male IUDR IGF-1 was 38% less than male CON ($p < 0.001$). Male and female IPDR and PNDR IGF-1 was 90% less than their respective CON and IUDR groups ($p < 0.001$ for each). Female IPDR valine and isoleucine was 30% and 37% less than CON ($p < 0.007$ and 0.002 , respectively). While there were no differences in valine and isoleucine in the other male groups, leucine in male PNDR was 28% less than IUDR ($p = 0.03$). Examination of the rest of the amino acid profile revealed lower concentrations in the IPDR and PNDR groups when compared to CON,

being more pronounced in the females than in males in certain cases. The exception was threonine and aspartic acid in males and females, where no changes were observed in any groups (Table 2).

3.4 Skeletal Muscle Morphology

The postnatal d21 skeletal muscle morphology in both sexes of all four groups (Figure 3) and the quantification of the cross-sectional area of muscle bundles and fibers (Figure 4) are depicted. A significant diminution of at least 50% of both the cross-sectional areas of the bundles and fibers in IPDR and PNDR male (53%-67%) and female (53-68%) was observed when compared to CON and IUDR groups ($p<0.001$ for each). The female IUDR skeletal muscle bundle was smaller than male IUDR by about 11% ($p=0.01$), while the female CON muscle fiber was 29% bigger than male CON ($p=0.004$). Visual assessment demonstrated intra-muscular fat deposition in IUDR and IPDR female muscle when compared to CON (Figure 5).

3.5 mTOR Signaling Pathway

No inter-group change was seen in total and p-mTOR and S6K1 concentrations in either males and females except for female IPDR total S6K1, which was 23% less than CON ($p=0.02$) (Figures 6 and 7 A-B). Upstream to mTOR, phosphorylated (p)-TSC2 in male and female IPDR and PNDR groups was less than IUDR, contributing to the diminution of p-TSC2/total TSC2 ratio. Specifically, male IPDR and PNDR p-TSC2 was approximately 60% less than IUDR ($p<0.05$ each) leading to a reduction in the p-TSC2/total TSC2 ratio in PNDR versus IUDR ($p<0.05$). Female IPDR and PNDR p-TSC2 was 50% less than CON and IUDR ($p<0.001$ each). Again, a significant reduction in the p-TSC2/total TSC2 ratio was observed. Female IPDR p-TSC2/total TSC2 was less than CON ($p=0.009$) and IUDR ($p<0.001$). Following this trend, female PNDR p-TSC2/total TSC2 ratio was less than IUDR ($p<0.001$) (Figures 6 and 7 C-D).

Despite the findings that mTOR remained unchanged when the four groups were compared, downstream to mTOR, p-rS6 was 52-80% less in male IPDR and PNDR when compared to CON and IUDR ($p<0.05$ each). Male IPDR and PNDR p-rS6/total rS6 ratio was also less than CON by 82% and 70%, respectively ($p=0.001$ and 0.005, respectively). This decrease was less notable in the females where the ratio was 51% less in PNDR when compared to CON ($p=0.01$) (Figures 6 and 7E).

In contrast, while male IPDR and PNDR total 4EBP1 concentrations were greater than IUDR ($p<0.05$, respectively), no inter-group differences were observed with the p form or p to total protein ratio. Likewise, female IPDR total 4EPB1 was greater when compared than CON and IUDR ($p=0.008$ and 0.04, respectively) (Figures 6 and 7F). No changes were seen with total and p-eIF4E in males and females (Figures 6 and 7G).

Examination of p-MAPK and p-MAPK/MAPK revealed a significant increase in males, but no change in downstream p90RSK. In contrast, in females, MAPK was similar in all groups, but p-p90RSK and p-p90RSK/p90RSK revealed a significant decrease.

Specifically, male IPDR and PNDR p-MAPK demonstrated a 1.1–1.5-fold increase versus CON ($p=0.01$ and 0.04 , respectively). This led to a 1.1–1.3-fold increase in male IPDR and PNDR p-MAPK/MAPK versus CON ($p=0.02$ and 0.04 , respectively) (Figure 6H and I). Female MAPK was unchanged, but IPDR p-p90RSK was 28–43% less than CON and IUDR ($p=0.01$ and 0.04 , respectively). This led a 43% reduction in IPDR p-p90RSK/total p90RSK versus CON ($p=0.01$) (Figure 7H and I).

A summary of the data are presented in Table 3 and Figure 8. The findings for plasma glucose and amino acids are shown in Table 3. A graphic presentation of changes induced by postnatal dietary restriction in hindlimb skeletal muscle is presented in Figure 8.

4. Discussion

In a rat model, we investigated the effects of early dietary restriction on skeletal muscle morphology and mTOR. Prenatal dietary restriction led to growth restriction surmised by postnatal d21 body weights. In the IUDR group, post-parturient access to an *ad libitum* diet led to postnatal catch up growth by d21. When compared to CON, IUDR had comparable skeletal muscle mass. Moreover, we did not observe any significant changes in the mTOR signaling pathway when IUDR was compared to CON. However, post-parturient diet restriction, either alone or superimposed on prenatal diet restriction (PNDR and IPDR), culminated in postnatal growth restriction in both sexes. When compared to CON and IUDR, IPDR and PNDR exhibited a reduction in d21 body weights; diminution of skeletal muscle mass and most organ weights; and reduction in circulating glucose, IGF-1, and amino acid concentrations. We hypothesized that the offspring of mothers who were subjected to this type of dietary restriction would have reduced skeletal muscle mass and an attenuation in skeletal muscle mTOR when compared to control animals. However, despite a reduction in skeletal muscle mass, mTOR signaling remained intact in IPDR and PNDR when compared to CON.

While our results refute our hypothesis, the effects of dietary restriction on mTOR signaling are complex [16–20,27–29]. An important mTOR regulatory pathway is the low energy activated AMP kinase, which phosphorylates TSC2, which then complexes with TSC1, inhibiting mTOR [19,20,29]. Our investigation demonstrated a consistent reduction in p-TSC2 in males and females. This imbalance in the TSC1/TSC2 complex may have reduced inhibition of mTOR in the IPDR and PNDR groups. We were unable to measure p-AMP kinase in our studies. We speculate this may be secondary to low levels of p-AMP kinase in postnatal muscle. It remains unclear if we would detect a difference in p-AMP kinase if the animals were subjected to insulin or another stimulus [8,9,17,18]. Another important mTOR regulatory pathway is PI-3-kinase/Akt [19,20]. Activated Akt inhibits TSC2 phosphorylation, which in turn prevents formation of the inhibitory TSC1/TSC2 heterodimer activating mTOR. We have previously demonstrated enhanced post-insulin receptor signaling which included activation of Akt, a downstream target of insulin and growth factors in adult IPDR and PNDR [24]. For these reasons, we speculate that mTOR remained unchanged in IPDR and PNDR, escaping the expected inhibition in response to dietary restriction.

Downstream to mTOR are two signaling pathways, the S6K1, which is responsible for ribosomal biogenesis, and 4EBP1, which releases eIF4E thereby promoting 5'-cap dependent mRNA translation. Both these pathways also remained relatively unchanged, supporting the impact of the reduction of TSC2 not only on mTOR, but on the kinase-dependent and independent downstream mTOR signaling pathways. Despite this, a reduction in rS6 in IPDR and PNDR, more so in males than females, was observed. This observation may be secondary to a non-mTOR related mechanism independent of S6K1 [22,27]. Thus, while rS6 protein mediated ribosomal biogenesis may be negatively affected by dietary restriction, the mTOR pathway remained largely intact.

Ribosomal S6 protein activation is affected by other mechanisms besides S6K1 [21,22,27]. These pathways include the MAPK/ERK pathways, both regulated by insulin and/or IGFs involved in cell growth [22,27]. In the case of skeletal muscle, myogenesis consists of myoblast proliferation and myotube differentiation. While the mTOR pathway regulates the myotube maturation rather than myoblast proliferation, MAPK is intricately involved in myoblast proliferation [21]. Given this, in our present study, it is quite possible that other pathways in response to decreased IGFs may be responsible for rS6 protein suppression in the PNDR and IPDR groups. Examination of the MAPK pathway revealed enhanced activation of MAPK in male PNDR and IPDR when compared to CON, despite a decrease in glucose and IGF-1 concentrations. Regardless, this activation failed to reveal a change in the downstream activation of p90RSK, which is responsible for activating rs6 protein. Thus, in males, it appears that MAPK induction may represent a compensatory change in response to decreased nutrient provisions. Moreover, there may be a signaling disconnect at the level of MAPK and downstream p90RSK. A similar block at the level of PKCC downstream of activated Akt was previously reported in adult PNDR and IPDR [24]. In contrast, upstream, activated MAPK is known to inhibit TSC2 activation. Thus, activated MAPK in PNDR and IPDR males may contribute towards the inhibition of TSC2 and explain why mTOR remained unchanged despite dietary restriction.

Downstream, reduction in rS6 protein mediated ribosomal biogenesis ultimately has a negative impact on protein synthesis and skeletal muscle health [21,30]. A compensatory increase in the total 4EBP1 protein amounts was seen in PNDR and IPDR. However, no change in the phosphorylation of 4EBP1 resulted in a lack of change in total and phosphorylated amounts of eIF4E.

Our detection of intramyocyte fat deposition in female IUDR and IPDR is suggestive of a depletion of satellite cells in replenishing the damaged myofibers necessary for the required tensile strength of skeletal muscle [5,17]. We also observed a reduction in the cross-sectional area of muscle bundles and fibers in IPDR and PNDR. Lack of lean body mass has detrimental consequences. Besides contributing to muscle weakness, poor muscle development has the propensity of promoting the subsequent development of insulin resistance. When nutrients are re-routed away from skeletal muscle to white adipose tissue and other organs, central adiposity and the metabolic syndrome develop [1-5,30]. In this study, we observed that female IUDR white adipose tissue weighed more than their male counterparts, and female IUDR liver weighed more than CON. Longitudinal studies have demonstrated that fetal growth restriction followed by rapid weight gain during childhood is

associated with the development of non-alcoholic fatty liver disease and the metabolic syndrome [1,31]. It remains unknown how sex affects these outcomes.

Our study has demonstrated that postnatal dietary restriction (PNDR), alone or in combination with prenatal dietary restriction (IPDR), has detrimental effects on the growth trajectory and muscle development of the male and female offspring. With respect to mTOR signaling, dietary restriction did not decrease mTOR. However, a decrease in TSC2 and increase in MAPK may explain these findings.

This study has some limitations. The effects of nutrient deprivation may be muscle specific [28]. In these experiments, we studied soleus and gastrocnemius. As a result, it remains unclear if our results would be different if we examined slow twitch and fast twitch fibers separately [28]. Our polynutrient dietary restriction model may also be a limitation. However, polynutrient restriction is commonly encountered in the neonatal clinical setting where appropriate for gestational age and IUDR neonates are subjected to dietary restriction secondary to critical illness. These dietary restrictions can increase one's risk for the metabolic syndrome [1–5]. In our study, the prenatal dietary restriction induced insult (IUDR) was easily reversed by the postnatal introduction of sufficient nutrition. However, this detriment persists in the IPDR group, which mimics the PNDR phenotype. In this model, it remains unknown how the muscle phenotype would evolve if the IPDR and PNDR groups were given specific supplements (i.e., protein or micronutrients) during or after dietary restriction or *ad libitum* access to food after 21 days [32]. Our previous investigation reveals that both IPDR and PNDR adult offspring remain stunted in growth at 17 months even though the skeletal muscle morphology was not explored [9]. Because this study's nutritional deprivation occurred during a critical phase of development, we speculate that there could be long-term changes in skeletal muscle. In medicine, this could have potentially far-reaching health consequences—such as the metabolic syndrome—which can begin to manifest in childhood and then fully unravel in the adult years [1–7]. Further investigation of the TSC2, MAPK, and rS6 proteins offers possibilities for future therapeutic targeting to overcome poor muscle development seen with postnatal stunting, and its potential contribution towards the later development of insulin resistance.

Acknowledgments

We thank Pinchas Cohen (UCLA) for performing the IGF-1 enzyme-linked immunosorbent assays. This work was supported by Grants from the NIH (41230, 25024 and 081206 to SUD and T32HD0754 and K12HD001400 to KLC). The funding source had no involvement in this study. There are no declarations of interest.

Abbreviations

4EBP1	4E binding protein-1
AMP	adenosine monophosphate-activated protein
CON	control
eIF4E	eukaryotic translational initiation factor-4E
IGF	insulin-like growth factor

IPDR	postnatal dietary restriction
IUDR	dietary restriction
mTOR	mammalian target of rapamycin
MAPK	mitogen-activated protein kinase
NC	no change
p	phosphorylated
PNDR	postnatal dietary restriction
rs6	ribosomal s6
p90RSK	p90 ribosomal S6 kinase
S6K1	p70S6kinase-1
TSC	tuberous sclerosis complex

References

1. Calkins K, Devaskar SU. Fetal origins of adult disease. *Curr Probl Pediatr Adolesc Health Care*. 2011 Jul;41:158–76. [PubMed: 21684471]
2. Saleem T, Sajjad N, Fatima S, Habib N, Ali SR, Qadir M. Intra-uterine growth retardation--small events, big consequences. *Ital J Pediatr*. 2011 Sep;7:37–41.
3. Law CM, Barker DJ, Osmond C, Fall CH, Simmonds SJ. Early growth and abdominal fatness in adult life. *J Epidemiol Community Health*. 1992 Jun;46:184–6. [PubMed: 1645067]
4. Yliharsila H, Kajantie E, Osmond C, Forsen T, Barker DJ, Eriksson JG. Birth size, adult body composition and muscle strength in later life. *Int J Obes (Lond)*. 2007 Sep;31:1392–9. [PubMed: 17356523]
5. Brown LD. Endocrine regulation of fetal skeletal muscle growth: impact on future metabolic health. *J Endocrinol*. 2014 May;221:R13–29. [PubMed: 24532817]
6. Jimenez-Chillaron JC, Hernandez-Valencia M, Lightner A, Faucette RR, Reamer C, Przybyla R, et al. Reductions in nutrient intake and early postnatal growth prevent glucose intolerance and obesity associated with low birthweight. *Diabetologia*. 2006 Aug;49:1974–84. [PubMed: 16761107]
7. Roghair RD, Aldape G. Naturally occurring perinatal growth restriction in mice programs cardiovascular and endocrine function in a sex- and strain-dependent manner. *Pediatr Res*. 2007 Oct;62:399–404. [PubMed: 17667847]
8. Dai Y, Thamotharan S, Garg M, Shin BC, Devaskar SU. Superimposition of postnatal nutrient restriction protects the aging male intra-uterine growth-restricted offspring from metabolic maladaptations. *Endocrinology*. 2012 Sep;153:4216–26. [PubMed: 22807491]
9. Garg M, Thamotharan M, Dai Y, Thamotharan S, Shin BC, Stout D, et al. Early postnatal nutrient restriction protects adult male intra-uterine growth-restricted offspring from obesity. *Diabetes*. 2012 Jun;61:1391–8. [PubMed: 22461568]
10. Garg M, Thamotharan M, Dai Y, Lagishetty V, Matveyenko AV, Lee WN, et al. Glucose intolerance and lipid metabolic adaptations in response to intra-uterine and postnatal nutrient restriction in male adult rats. *Endocrinology*. 2013 Jan;154:102–13. [PubMed: 23183174]
11. Garg M, Thamotharan M, Pan G, Lee PW, Devaskar SU. Early exposure of the pregestational intra-uterine and postnatal growth-restricted female offspring to a peroxisome proliferator-activated receptor- γ agonist. *Am J Physiol Endocrinol Metab*. 2009 Mar;298:E489–98. [PubMed: 20009032]

12. Ganguly A, Collis L, Devaskar SU. Placental glucose and amino acid transport in nutrient-restricted wild-type and Glut3 null heterozygous mice. *Endocrinology*. 2012 Aug.153:3995–4007. [PubMed: 22700768]
13. Jansson T, Ylven K, Wennergren M, Powell TL. Glucose transport and system A activity in syncytiotrophoblast microvillous and basal plasma membranes in intra-uterine growth restriction. *Placenta*. 2002 May.23:392–9. [PubMed: 12061855]
14. Bhasin KK, van Nas A, Martin LJ, Davis RC, Devaskar SU, Lusic AJ. Maternal low-protein diet or hypercholesterolemia reduces circulating essential amino acids and leads to intra-uterine growth restriction. *Diabetes*. 2009 Mar.58:559–66. [PubMed: 19073773]
15. Alexandre-Gouabau MC, Courant F, Le Gall G, Moyon T, Darmaun D, Parnet P, et al. Offspring metabolomics response to maternal protein restriction in a rat model of intrauterine growth restriction (IUGR). *J Proteome Res*. 2011 Jul 1; 10(7):3292–302. [PubMed: 21608999]
16. Williamson DL, Dungan CM, Mahmoud AM, Mey JT, Blackburn BK, Haus JM. Aberrant REDD1-mTORC1 responses to insulin in skeletal muscle from Type 2 diabetics. *Am J Physiol Regul Integr Comp Physiol*. 2015 Oct 15; 309(8):R855–63. [PubMed: 26269521]
17. Rivas DA, McDonald DJ, Rice NP, Haran PH, Dolnikowski GG, Fielding RA. Diminished anabolic signaling response to insulin induced by intramuscular lipid accumulation is associated with inflammation in aging but not obesity. *Am J Physiol Regul Integr Comp Physiol*. 2016 Apr; 310(7):R561–9. [PubMed: 26764052]
18. Dungan CM, Williamson DL. Regulation of skeletal muscle insulin-stimulated signaling through the MEK-REDD1-mTOR axis. *Biochem Biophys Res Commun*. 2017 Jan; 482(4):1067–1072. [PubMed: 27913296]
19. Mee-Sup, Yoon. mTOR as a key regulator in maintaining skeletal muscle mass. *Front Physiol*. 2017; 8:788. [PubMed: 29089899]
20. Wullschleger S, Loewith R, Hall MN. TOR signaling in growth and metabolism. *Cell*. 2006 Feb. 124:471–84. [PubMed: 16469695]
21. Schiaffino S, Dyar KA, Ciciliot S, Blaauw B, Sandri M. Mechanisms regulating skeletal muscle growth and atrophy. *FEBS J*. 2013 Sep.280:4294–314. [PubMed: 23517348]
22. Anjum R, Blenis J. The RSK family of kinases: emerging roles in cellular signaling. *Nat Rev Mol Cell Biol*. 2008 Oct.9:747–58. [PubMed: 18813292]
23. [accessed 12 January 2018] <http://www.envigo.com/resources/data-sheets/7013-datasheet-0915.pdf>
24. Oak SA, Tran C, Pan G, Thamotharan M, Devaskar SU. Perturbed skeletal muscle insulin signaling in the adult female intra-uterine growth-restricted rat. *Am J Physiol Endocrinol Metab*. 2006 Jun. 290:E1321–30. [PubMed: 16449300]
25. Muzumdar RH, Ma X, Fishman S, Yang X, Atzmon G, Vuguin P, et al. Central and opposing effects of IGF-I and IGF-binding protein-3 on systemic insulin action. *Diabetes*. 2006 Oct; 55(10): 2788–96. [PubMed: 17003344]
26. Kalhan SC, Guo L, Edmison J, Dasarathy S, McCullough AJ, Hanson RW, et al. Plasma metabolomic profile in nonalcoholic fatty liver disease. *Metabolism*. 2011 Mar; 60(3):404–13. [PubMed: 20423748]
27. Sharma N, Bhat AD, Kassa AD, Xiao Y, Arias EB, Cartee GD. Improved insulin sensitivity with calorie restriction does not require reduced JNK1/2, p38, or ERK1/2 phosphorylation in skeletal muscle of 9-month-old rats. *Am J Physiol Regul Integr Comp Physiol*. 2012 Jan; 302(1):R126–36. [PubMed: 22012698]
28. Sharma N, Castorena CM, Cartee GD. Tissue-specific responses of IGF-1/Insulin and mTOR signaling in calorie restricted rats. *PLoS One*. 2012; 7(6):e38835. [PubMed: 22701721]
29. Inoki K, Zhu T, Guan KL. TSC2 mediates cellular energy response to control cell growth and survival. *Cell*. 2003 Nov.115:577–90. [PubMed: 14651849]
30. Srikanthan P, Karlamangla AS. Relative muscle mass is inversely associated with insulin resistance and prediabetes. Findings from the third National Health and Nutrition Examination Survey. *J Clin Endocrinol Metab*. 2011 Sep.96:2898–903. [PubMed: 21778224]
31. Nobili V, Alisi A, Panera N, Agostoni C. Low birth weight and catch-up-growth associated with metabolic syndrome: a ten year systematic review. *Pediatr Endocrinol Rev*. 2008 Dec; 6(2):241–7. [PubMed: 19202511]

32. Teodoro GF, Vianna D, Torres-Leal FL, Pantaleao LC, Matos-Neo EM, Donato J Jr, et al. Leucine is essential for attenuating fetal growth restriction caused by a protein-restricted diet in rats. *J Nutr.* 2012 May; 142(5):924–30. [PubMed: 22457392]

Author Manuscript

Author Manuscript

Author Manuscript

Author Manuscript

Highlights

- In rat skeletal muscle, postnatal dietary restriction reduces muscle mass, but does not alter the mammalian target of rapamycin (mTOR).
- Postnatal dietary restriction reduces TSC2, which may explain why mTOR remains unchanged.
- In males subjected to postnatal dietary restriction, an increase in mitogen-activated protein kinase (MAPK) and decrease in ribosomal (rs6) suggests a possible block in MAPK signaling.

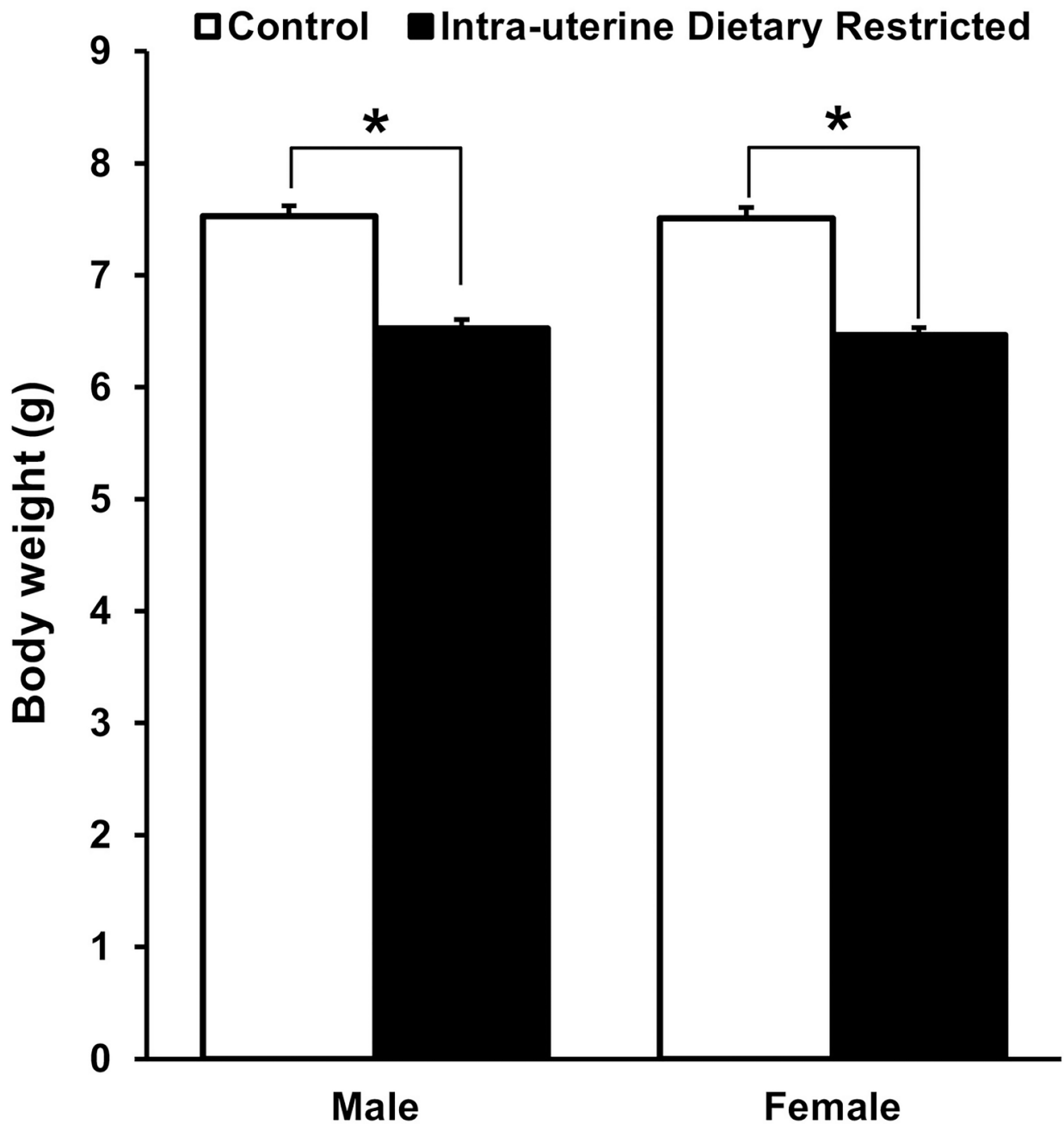


Figure 1. Rat day 2 body weights for control and dietary restricted males and females
Values are means \pm SEM, n=72 pups for male control group, n=77 pups for male intra-uterine dietary restricted group, n=63 pups for female control group, and n=63 female intra-uterine dietary restricted group. *p<0.001 (Student t-test).

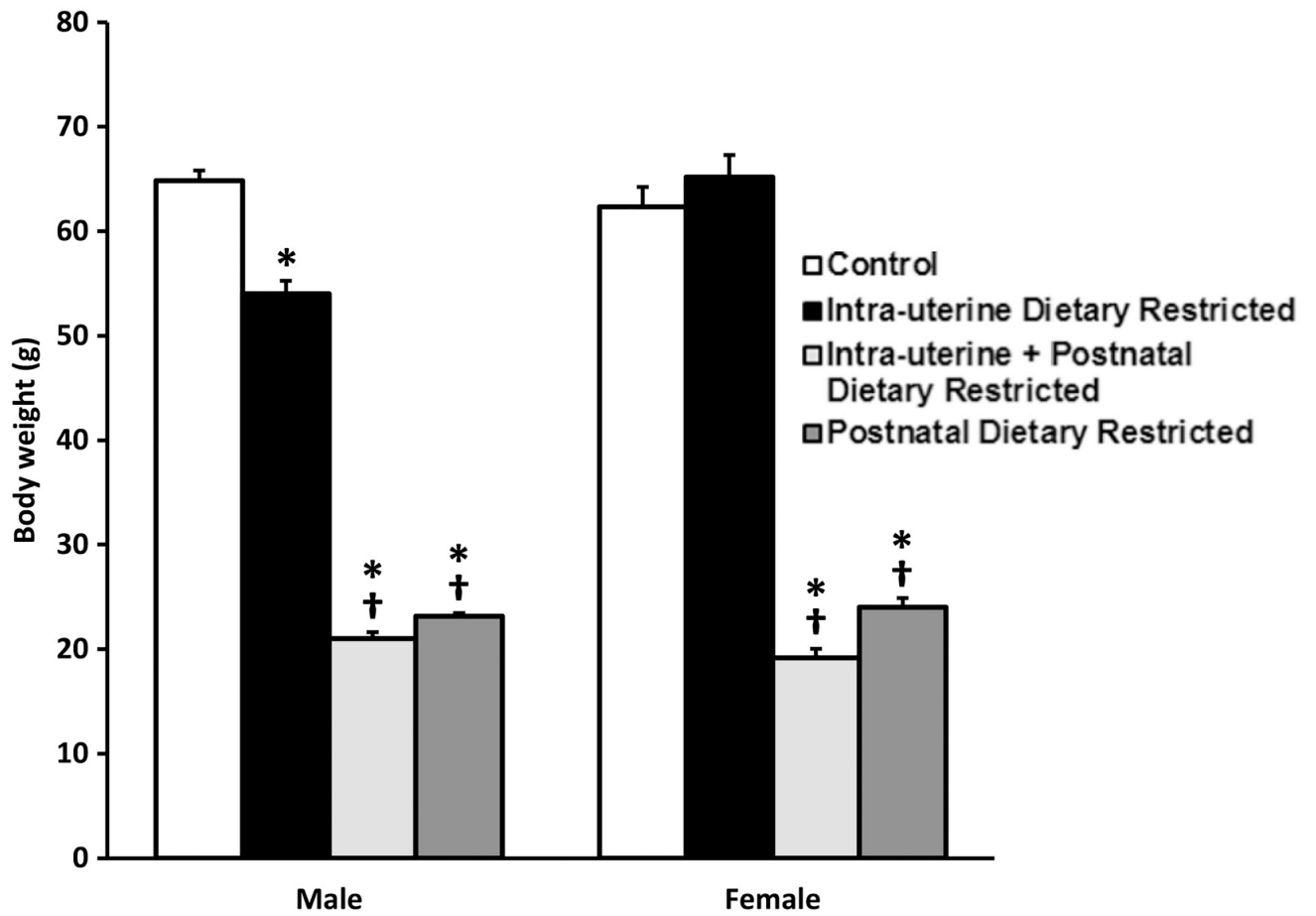


Figure 2. Rat day 21 body weights for control and dietary restricted males and females
Values are means \pm SEM. n=6 pups/group, *p<0.001 vs. control, †p<0.001 vs. intra-uterine dietary restricted (two-way analysis of variance model with a post-hoc Tukey test).

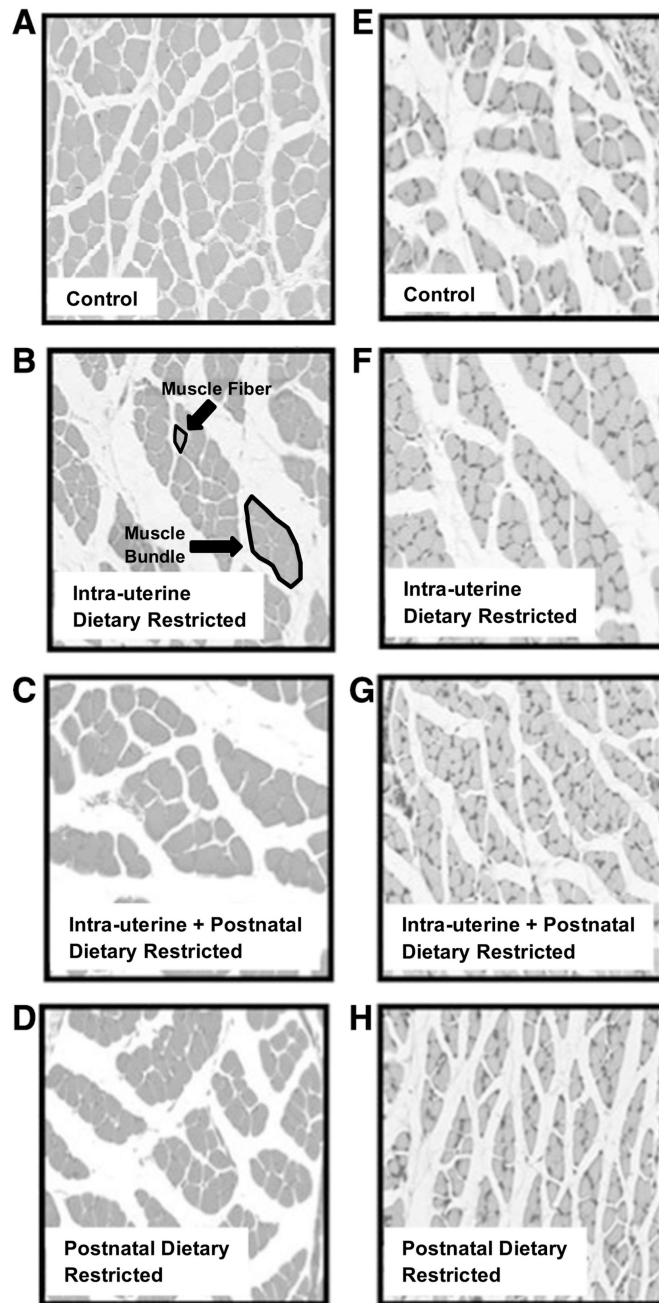


Figure 3. Soleus muscle morphology for day 21 control and dietary restricted male (A–D) and female (E–H) rats
Magnification, 20 \times .

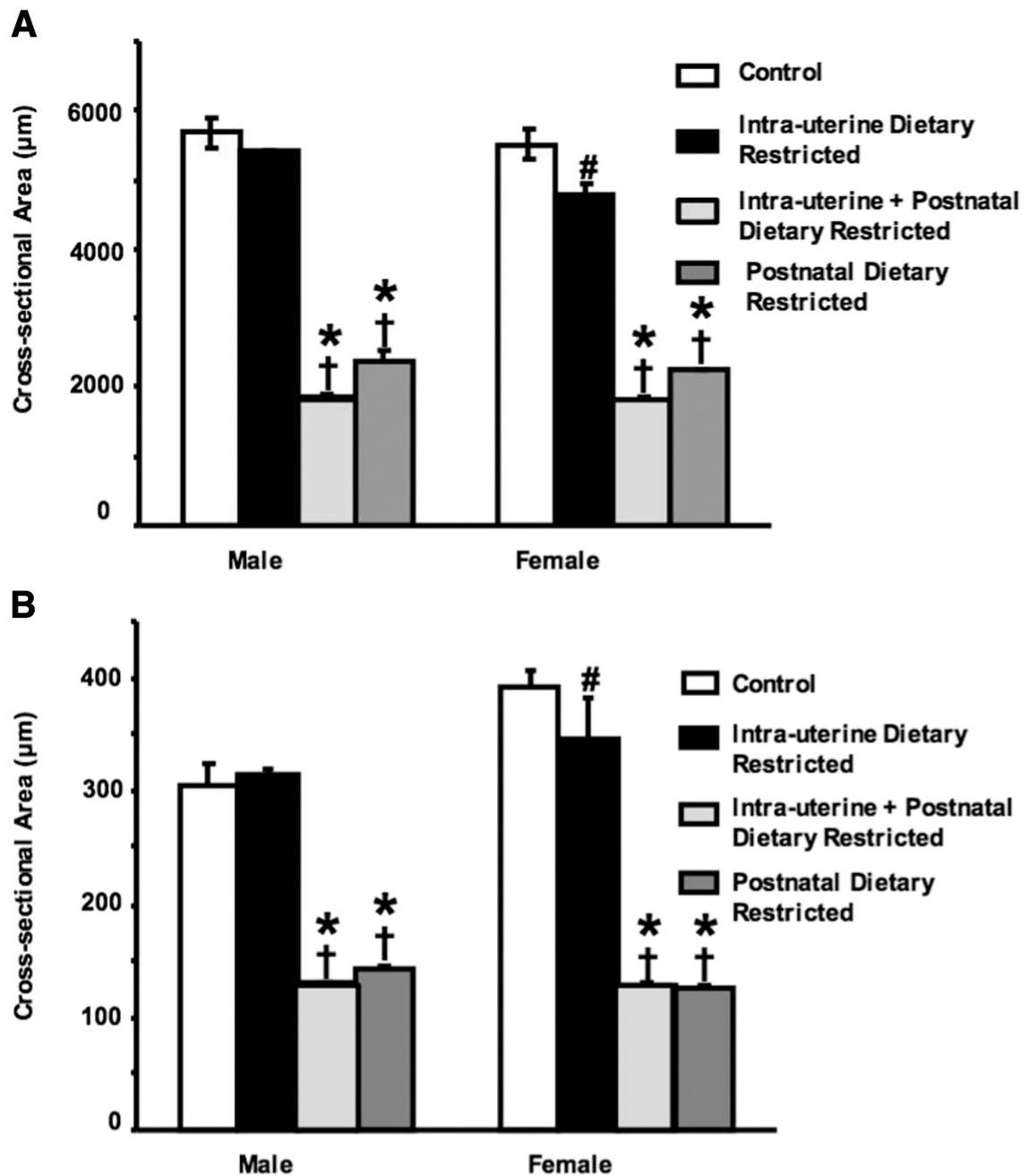


Figure 4. Cross-sectional area of muscle bundle (A) and fiber (B) for day 21 control and dietary restricted male and female rats

Values are means \pm SEM. n=3 pups (2–6 measurements per pup). *p<0.001 vs. control, †p<0.001 vs. intra-uterine dietary restricted, #p<0.05 vs. male (two-way analysis of variance model with a post-hoc Tukey test).

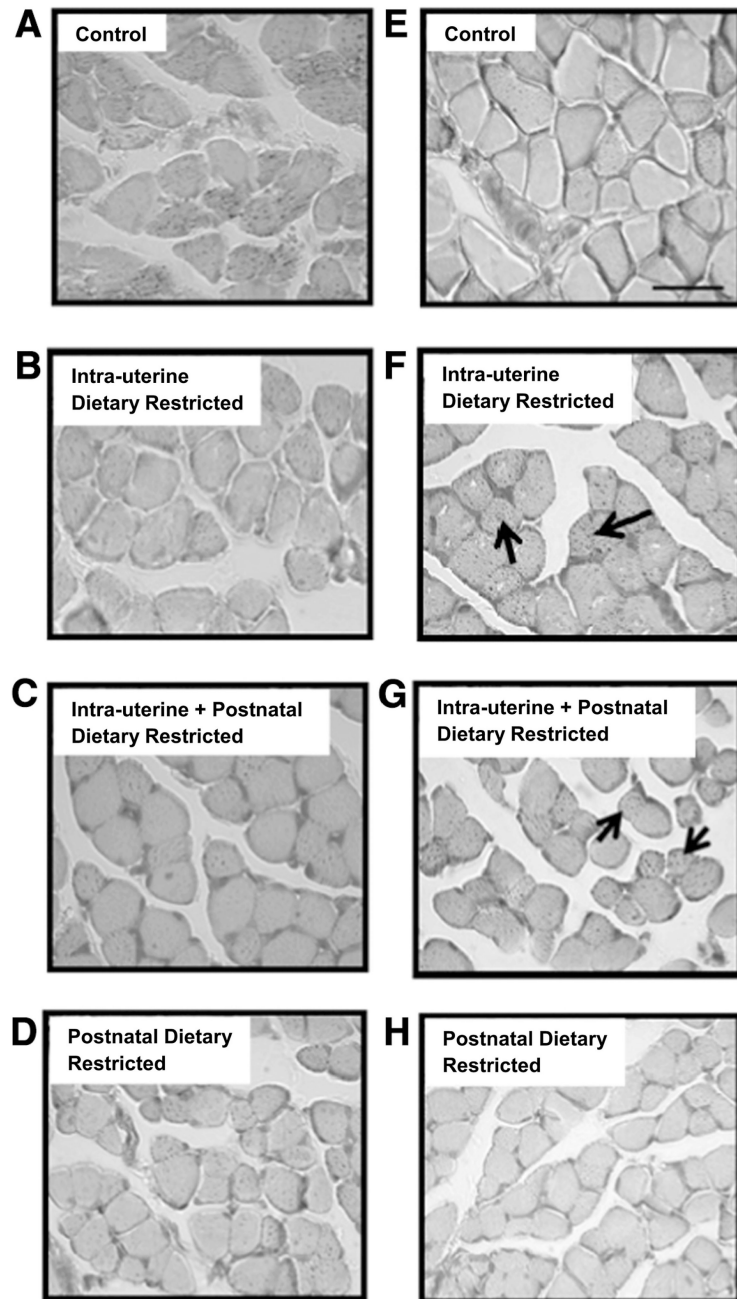


Figure 5. Soleus fat deposition in day 21 control and dietary restricted male (A–D) and female (E–H) rats
Fat deposits are shown with arrows. Scale bar shows magnification. Magnification, 40 \times .

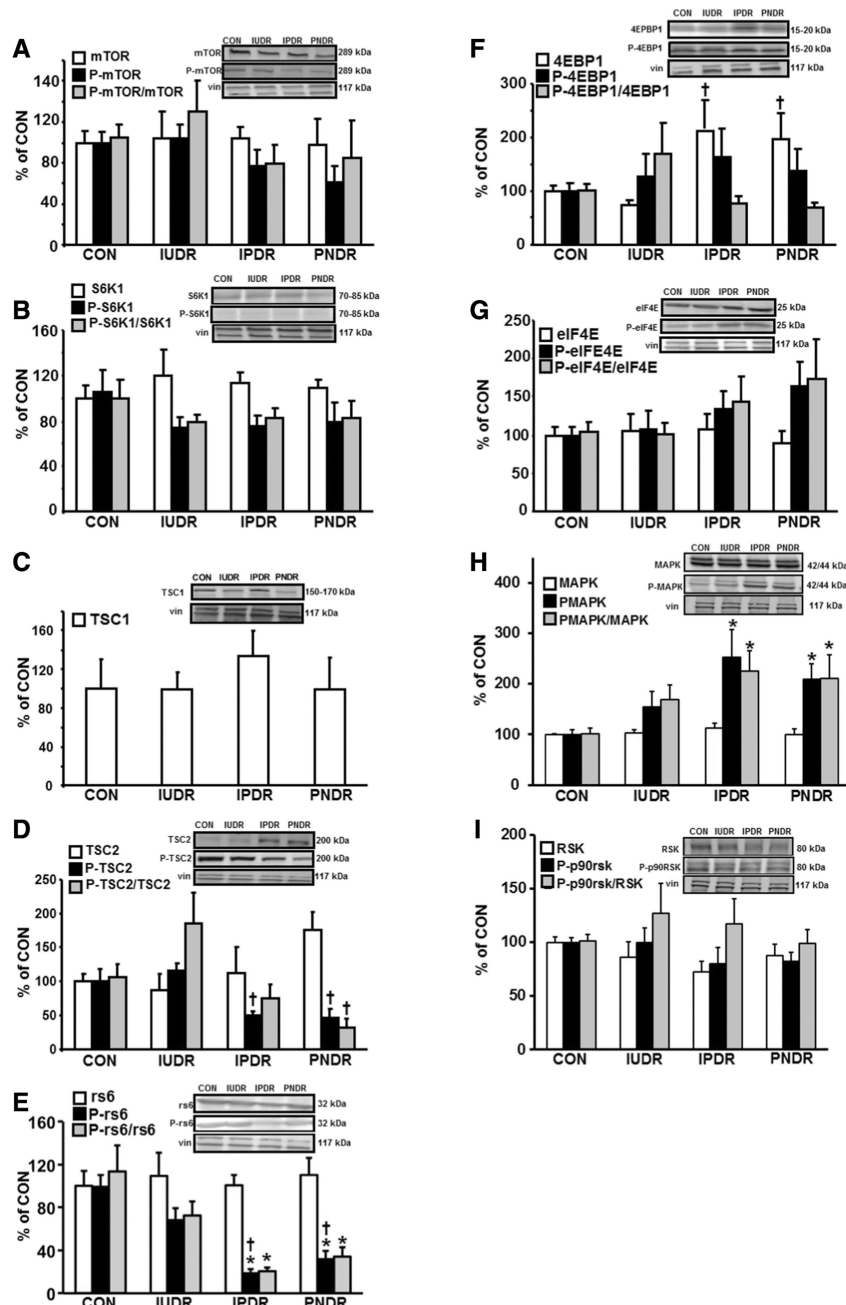


Figure 6. Skeletal muscle mTOR signaling pathway in day 21 control and dietary restricted male rats

Values are means \pm SEM. All data is presented as a % of control. n=6 pups/group, *p<0.05 vs. CON, †p<0.05 vs. IUDR (one-way analysis of variance model with a post-hoc Tukey test). Western blots depicted in the insets demonstrate total protein (top panel), phosphorylated (p) protein (middle panel) and internal loading control, vinculin (vin) (bottom panel). The bar graphs below show quantification of the proteins. Mammalian target of rapamycin (mTOR) (A), p70S6K1 (S6K1) (B), tuberous sclerosis complex (TSC)-1 (C), TSC2 (D), ribosomal s6 (rS6) (E), 4E-binding protein- 1 (4EBP1) (F) and elongation

initiation factor-4E (eIF4E) (**G**), mitogen activated protein kinase (MAPK) (**H**), p90 ribosomal S6 kinase (p90RSK) (**I**) total and p-protein along with the p-protein/total protein ratios are shown for control (CON), intra-uterine dietary restricted (IUDR), intra-uterine and postnatal dietary restricted (IPDR) and postnatal dietary restricted (PNDR) groups.

Author Manuscript

Author Manuscript

Author Manuscript

Author Manuscript

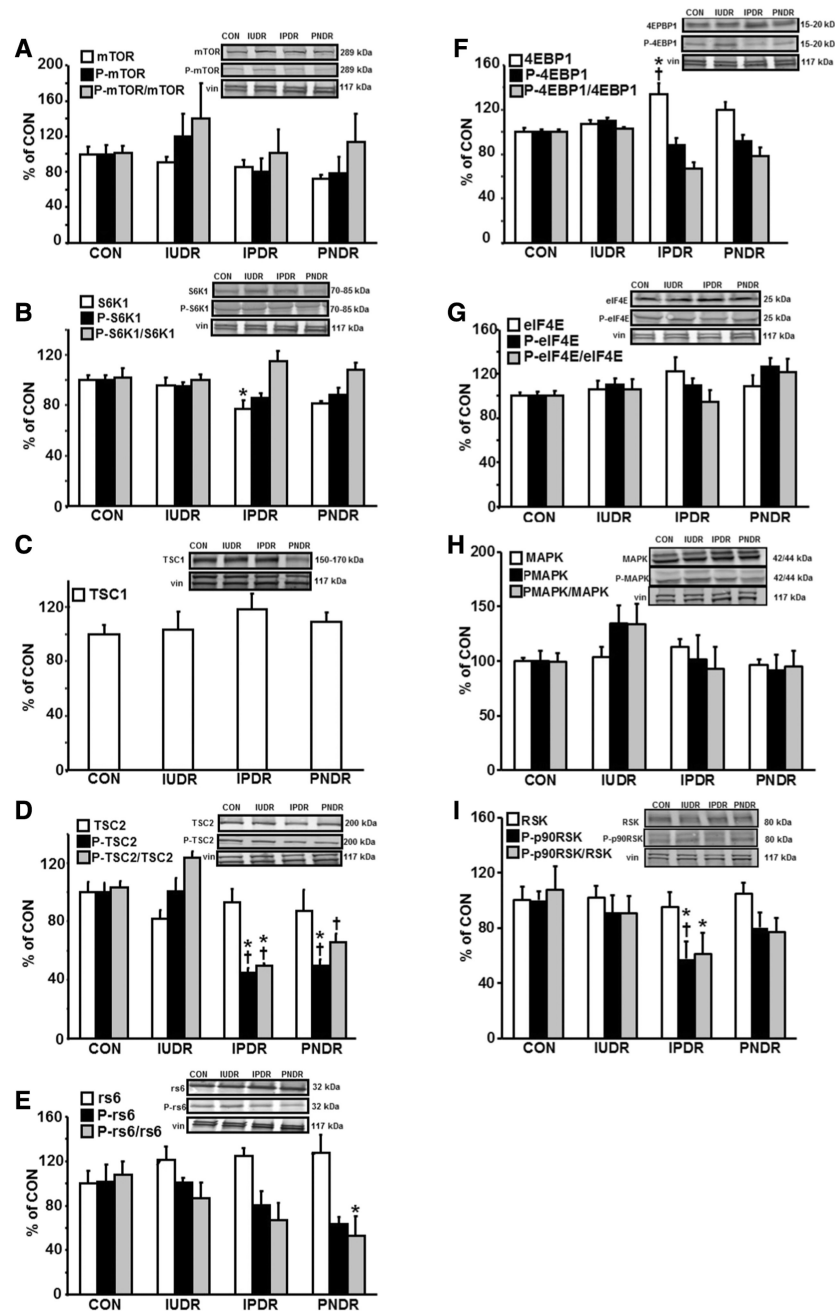


Figure 7. Skeletal muscle mTOR signaling pathway in day 21 control and dietary restricted female rats

Values are means±SEM. All data is presented as a % of control. n=6 pups/group, *p<0.05 vs. CON, †p<0.05 vs. IUDR (one-way analysis of variance model with a post-hoc Tukey test). Western blots depicted in the insets demonstrate total protein (top panel), phosphorylated (p) protein (middle panel) and internal loading control, vinculin (vin) (bottom panel). The bar graphs below show quantification of the proteins. Mammalian target of rapamycin (mTOR) (A), p70S6K1 (S6K1) (B), tuberous sclerosis complex (TSC)-1 (C), TSC2 (D), ribosomal s6 (rS6) (E), 4E-binding protein- 1 (4EBP1) (F) and elongation

initiation factor-4E (eIF4E) (**G**), mitogen activated protein kinase (MAPK) (**H**), p90 ribosomal S6 kinase (p90RSK) (**I**) total and p-protein along with the p-protein/total protein ratios are shown for control (CON), intra-uterine dietary restricted (IUDR), intra-uterine and postnatal dietary restricted (IPDR) and postnatal dietary restricted (PNDR) groups.

Author Manuscript

Author Manuscript

Author Manuscript

Author Manuscript

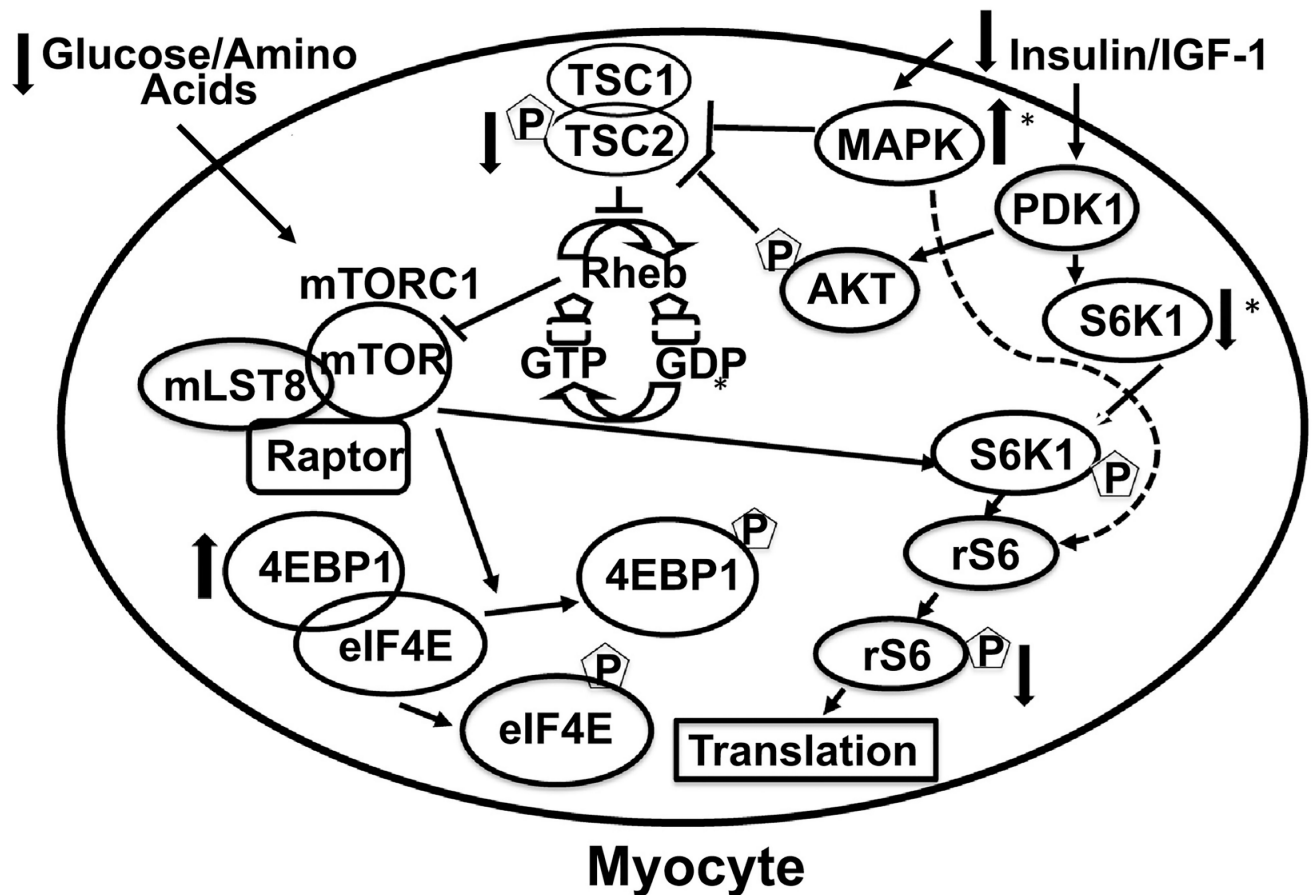


Figure 8. Summary of changes induced by postnatal dietary restriction in hindlimb skeletal muscle of day 21 rats
 IGF, insulin-like growth factor; mTOR, mammalian target of rapamycin; TSC, tuberous sclerosis complex; S6K1, p70S6kinase-1; rs6; ribosomal s6; 4EBP1, 4E binding protein-1; eIF4E, eukaryotic translational initiation factor-4E; MAPK, mitogen-activated protein kinase; p, phosphorylated. *sex-specific changes noted.

Table 1

Anthropometric Measurements for Day 21 Control and Diet Restricted Rats

	Control		Intra-uterine Dietary Restricted		Intra-uterine + Postnatal Dietary Restricted		Postnatal Dietary Restricted	
	Male	Female	Male	Female	Male	Female	Male	Female
Brain, g	1.5±0.02	1.5±0.02	1.5±0.05	1.5±0.02	1.2±0.01*	1.2±0.02*	1.3±0.01*	1.3±0.02*
Brain/BW, mg/g	2.3±0.03	1.9±0.4	2.7±0.1	2.3±0.07	6±0.2*	6.5±0.3*	5.6±0.1*	5.4±0.1* [§]
Length, cm	21±0.3	21±0.02	19±0.2*	21±0.3 [#]	14.5±0.3*	16±0.2*	15±0.3*	16±0.2* [#]
Length/BW, cm/g	0.32±0.01	0.34±0.01	0.36±0.01	0.03±0.01	0.69±0.01*	0.78±0.03* [#]	0.65±0.01*	0.68±0.02* [§]
Liver, g	2.7±0.06	2.1±0.1 [#]	2.2±0.09*	2.9±0.2* [#]	0.6±0.02*	0.6±0.01*	0.7±0.02*	0.7±0.03*
Liver/BW, mg/g	4.2±0.07	3.5±0.1 [#]	4±0.09	4.5±0.2* [#]	2.9±0.07*	3.3±0.2 [†] #	3±0.05*	2.9±0.4*
Kidney, g	0.8±0.03	0.7±0.02	0.6±0.02*	0.7±0.01 [#]	0.3±0.01*	0.3±0.001*	0.3±0.01*	0.3±0.01*
Kidney/BW, mg/g	1.2±0.03	1.2±0.03	1.1±0.03	1.1±0.03	1.3±0.03 [†]	1.4±0.07* [#]	1.3±0.04*	1.3±0.04 [†]
Pancreas, g	0.3±0.01	0.3±0.02	0.2±0.01*	0.3±0.02 [#]	0.1±0.01*	0.1±0.01*	0.1±0.02*	0.2±0.01*
Pancreas/BW, mg/g	0.4±0.01	0.5±0.03	0.4±0.02	0.5±0.03	0.5±0.05	0.8±0.07* [#]	0.5±0.09 [†]	0.6±0.04
White Adipose Tissue, g	0.3±0.02	0.4±0.03	0.2±0.02	0.5±0.06* [#]	--	--	--	--
White Adipose Tissue/BW, mg/g	0.5±0.03	0.7±0.04 [#]	0.5±0.03	0.7±0.07 [#]	--	0.1±0.01	--	--
Brown Adipose Tissue, g	0.3±0.02	0.3±0.02	0.2±0.03	0.1±0.04*	0.03±0.01*	0.06±0.01*	0.03±0.01*	0.06±0.01* [#]
Brown Adipose	0.4±0.03	0.4±0.04	0.4±0.06	0.3±0.05	0.1±0.03*	0.2±0.02*	0.1±0.03*	0.1±0.04*
Soleus, mg	27±0	22±1.7 [#]	24±2	21±2.7	6±0.3*	5.7±0.3*	9±0.3*	5.3±0.7*
Soleus/BW, mg ³ /g ³	0.5±0.01	0.4±0.03	0.5±0.1	0.4±0.04	0.5±0.03	0.3±0.01	0.4±0.02	0.3±0.05
Gastrocnemius, g	0.6±0.07	0.8±0.05 [#]	0.4±0.01*	0.7±0.07 [#]	0.2±0.01*	0.2±0.02*	0.1±0.01*	0.3±0.02* [#]
Gastrocnemius/BW, mg/g	0.9±0.1	1.2±0.1 [#]	0.7±0.03	1.1±0.1 [#]	0.7±0.04	1.2±0.1 [#]	0.8±0.04	1.3±0.1 [#]

Values are means±SEM, n=6 pups/group with the exception of male control and female postnatal dietary restricted for gastrocnemius (n=5 pups/group) and soleus (n=3 pups/group) and soleus/BW (n=3 pups/group)

* p<0.05 vs. control

[†] p<0.05 vs. intra-uterine dietary restricted

[§] p<0.05 vs. intra-uterine and postnatal dietary restricted

p<0.05 vs. male (2-way analysis of variance model with a post-hoc Tukey test). BW, body weight.

Author Manuscript

Author Manuscript

Author Manuscript

Author Manuscript

Table 2
Plasma Glucose, IGF-1, and Amino Acid Concentrations for 21 Day Control and Diet Restricted Rats

	Control		Intra-uterine Dietary Restricted		Intra-uterine + Postnatal Dietary Restricted		Postnatal Dietary Restricted	
	Male	Female	Male	Female	Male	Female	Male	Female
Glucose, mg/dL	162±6	184±9	149±10	168±13	109±2*	112±4*	125±7*	121±7*
IGF-1, ng ² /dL	460±29	318±39#	288±30*	352±29	12±2*	27±3*	11±2* [†]	32±5*
Isoleucine (µl)	74±3	92±5	82±7	82±3	73±2	58±9*	58±2	76±4
Leucine (µl)	151±6	172±13	175±13	156±5	139±3	127±19	126±5 [†]	154±5
Threonine (µl)	152±10	192±6	145±11	179±4	132±12	149±23	153±6	151±8
Methionine (µl)	55±1	93±5#	57±4	79±6#	28±1*	28±4*	28±1*	33±1*
Lysine (µl)	185±30	362±15#	185±21	343±30#	242±17	210±37*	319±23*	206±25*
Tryptophan (µl)	78±3	66±5	60±4*	51±3*	34±1*	23±4*	28±2*	22±1*
Phenylalanine (µl)	77±1	79±4	83±7	71±3	57±2*	59±4*	66±3	65±2
Glutamic acid (µl)	92±3	109±18	100±5	114±8	65±2	188±104	63±6	61±10
Asparagine (µl)	97±4	106±10	99±2	101±4	45±2*	40±11*	35±2*	41±3*
Serine (µl)	523±12	352±30#	499±14	321±18#	269±8*	189±35*	248±15*	212±20*
Glutamine (µl)	769±27	655±60	807±19	622±22#	476±25*	378±52*	506±24*	387±20*
Glycine (µl)	786±50	409±10#	836±46	397±17#	459±15*	329±22	530±25*	368±19#
Histidine (µl)	143±5	111±12	146±7	96±4#	79±2*	61±12*	76±3*	66±5*
Alanine (µl)	734±37	618±68	768±42	566±13#	240±7*	220±50*	236±15*	200±13*
Taurine (µl)	216±9	382±37	159±8	389±9#	174±9	366±92#	228±24	254±30
Tyrosine (µl)	127±3	104±5±	143±7	99±3±	54±6* [†]	50±5* [†]	53±4* [†]	51±2* [†]
Arginine (µl)	306±7	316±10	285±16	319±16	157±6* [†]	162±27* [†]	183±9* [†]	208±27* [†]
Aspartic acid (µl)	24±1	29±5	26±2	27±1	27±1	101±51	28±3	27±2

[†] Values are means±SEM, n=6 pups/group with the exception of male postnatal dietary restricted for glucose and IGF-1 (n=5 pups/group).

* p<0.05 vs. control

[†] p<0.05 vs. intra-uterine dietary restricted

Author Manuscript

Author Manuscript

Author Manuscript

Author Manuscript

\$ p<0.05 vs. intra-uterine and postnatal dietary restricted

p<0.05 vs. male (2-way analysis of variance model with a post-hoc Tukey test). IGF; insulin-like growth factor.

Table 3

Results showing the degree of changes in glucose, IGF-1, amino acids, and proteins resulting from in intra-uterine and postnatal dietary restricted rats

	Intra-uterine + Postnatal Dietary Restricted		Postnatal Dietary Restricted	
	Male	Female	Male	Female
Glucose	↓* [†]	↓* [†]	↓* [†]	↓* [†]
IGF-1	↓* [†]	↓* [†]	↓* [†]	↓* [†]
Amino acids	↓* [†]	↓* [†]	↓* [†]	↓* [†]
mTOR	NC	NC	NC	NC
p-mTOR	NC	NC	NC	NC
p-mTOR/mTOR	NC	NC	NC	NC
S6K1	NC	↓*	NC	NC
p-S6K1	NC	NC	NC	NC
p-S6K1/S6K1	NC	NC	NC	NC
TSC1	NC	NC	NC	NC
TSC2	NC	NC	NC	NC
p-TSC2	↓ [†]	↓* [†]	↓ [†]	↓* [†]
p-TSC2/TSC1	NC	↓* [†]	↓* [†]	↓ [†]
rs6	NC	NC	NC	NC
p-rs6	↓* [†]	NC	↓* [†]	NC
p-rs6/rs6	↓*	NC	↓*	↓*
4EBP1	↑ [†]	↑*	↑ [†]	NC
p-4EBP1	NC	NC	NC	NC
p-4EBP1/4EBP1	NC	NC	NC	NC
eIF4E	NC	NC	NC	NC
p-eIF4E	NC	NC	NC	NC
p-eIF4E/eIF4E	NC	NC	NC	NC
MAPK	NC	NC	NC	NC
p-MAPK	↑*	NC	↑*	NC
p-MAPK/MAPK	↑*	NC	↑*	NC
p90RSK	NC	NC	NC	NC
p-p90RSK	NC	↓* [†]	NC	NC
p-p90RSK/p90RSK	NC	↓*	NC	NC

NC: no change

* p<0.05 vs. control

[†] p<0.05 vs. intra-uterine dietary restricted.